

Helical self-organization in 3D MHD modelling of fusion plasmas: plasma flow effects and Alfvén waves detection

M.Veranda¹, D.Bonfiglio¹, S.Cappello¹, L. Chacón², D.F.Escande³, A.Kryzhanovskyy¹, M.Zuin¹

¹*Consorzio RFX (CNR, ENEA, INFN, Università degli Studi di Padova, Acciaierie Venete SpA), Padova, Italy*

²*Los Alamos National Laboratory, Los Alamos, New Mexico, USA*

³*Aix-Marseille Univ, CNRS, PIIM, UMR 7345, Marseille, France*

Introduction: Self-organized helical states and plasma rotation are observed ubiquitously in magnetically confined plasmas. Helical states can form in the core of tokamaks, associated with core MHD activity [1,2] and can include the whole plasma in the reversed-field pinch (RFP) configuration - where they are predicted by theory and observed in experiments [3]. Plasma rotation is subject of a vast literature, and we refer the reader to [4] for an excellent review of this subject. It consists of toroidal velocities of tens of km/s, measured both in tokamaks and RFPs, also in the absence of direct external momentum input; among other things it is involved in a mechanism of reduction of turbulent fluctuations of the magnetic field [5]. It can interact with external error fields and resonant magnetic perturbations in a rich variety of manner, classified in [6,7]. For example, toroidal rotation can be slowed down by an external field which penetrates in the plasma or, conversely, rotation can inhibit penetration of external magnetic field error, an effect enhanced at low plasma dissipation. **In this paper** we analyse the interplay of a small seed external magnetic perturbation and/or large self-organized helical states with a macroscopic plasma rotation, in the framework of 3D nonlinear MHD modelling in cylindrical geometry. First, we analyse the interplay between plasma rotation and error fields in tokamaks, in the so-called “forced reconnection” regime [6,7,8,9], confirming the screening of small error fields by plasma rotation, and the braking of bulk plasma rotation when the error field exceeds a threshold. Second, we consider plasma rotation in a 2D helical RFP and we sketch its impact on 3D self-organized RFP: we show examples of bulk plasma flow generation due to electromagnetic interaction between different MHD modes and that a moderate intensity of rotation can enhance of the quality of the helical state. Finally, we report for the first time the excitation of both compressional and shear Alfvén waves in nonlinear RFP modelling. **Numerical modelling:** Plasma is modelled as a single fluid, performing nonlinear visco-resistive MHD numerical simulations with the cylindrical and spectral code SpeCyl [10]. The model equations and

simulations setup are described in [3]. To carry out the analysis presented in this work we added a momentum source to the equation of motion to generate a bulk axisymmetric plasma flow in the axial direction, like in [11]. **2D Tokamak error fields / forced reconnection.** The first part of our work, devoted to the tokamak configuration, tests that our code is able to reproduce well-established results about the so-called “forced reconnection” regime in simple reference cases. We thus consider intrinsically tearing stable tokamak plasma, with zero β , in a cylinder. The interaction with an externally applied error field allows magnetic reconnection to take place, and thus the study of the interaction between magnetic islands and plasma flow. We start from a 1D Ohmic equilibrium with normalized resistivity $\eta_0=S^{-1}=10^{-6}$ increasing towards the edge and flat viscosity $\nu_0=M^{-1}=3 \cdot 10^{-5}$. We evolve a spectrum of 5 harmonics of the $m=2$, $n=-1$ mode (2D simulations). Reconnection is forced by imposing an external radial error field (Magnetic Perturbation, MP) with helicity $m=2, n=-1$ and amplitude $b_r(a)=10^{-4}$. Fig.1a shows the safety factor profile, the resonance is at $r_s/a=0.69$, and the magnetic island resulting from forced reconnection is shown in Fig.1b (associated to this magnetic island there is a typical flow and current density pattern). We show the reconnected error field at the resonance varying the intensity of the momentum source in Fig.1c. As bulk plasma rotation is increased up to $0.025v_A$ (Alfvén velocity, $v_A \approx 10^7$ m/s, depends on magnetic field and inverse square root of plasma density) the value of the reconnected flux decreases to around 20% of its value without plasma flow and the phase of the magnetic island generated by reconnection is shifted of $\pi/2$. A formula to describe such behavior can be inferred from [12] as $b_r(r_s) = (a + iv_{z0})^{-1}b_r(a)$. We now show the reciprocal phenomenon of bulk plasma rotation braking by imposing an increasing error field. Fig.2a shows that, as $b_r(a)$ is increased, the bulk velocity decreases from its unperturbed value to 30% of it. It is also interesting to analyze the role of visco-resistive dissipation in the penetration of the error field in the plasma. Fig.2b shows that decreasing resistivity and viscosity decreases the value of the reconnected error field, thus confirming previous results from 3D MHD [7]. **2D reversed-field pinch tearing reconnection.** The main difference between the tokamak and RFP behaviour is the tendency of the latter to shape its magnetic topology in a global helix, which interacts differently with the imposed bulk flow. We evolve a spectrum of 20 harmonics with $n/m=-10$, associated with unstable tearing (resistive-kink) modes. Fig.3a shows the safety factor profile, while Fig3b shows the helical flux surfaces topology after the helical MHD modes have grown, saturated and distorted the plasma column into a helical shape, with a dynamics shown in Fig.4a, where the temporal behaviour of the $m=1$ radial magnetic field is

shown ($\eta_0=10^{-4}$, $v_0=3 \cdot 10^{-4}$). In the simulation of Fig.4 an external momentum source is imposed, generating the initial axisymmetric flow profile shown in Fig.4c (blue parabolic profile). It interacts with the self-organized plasma in two ways. First, it puts the helical core in rotation, as seen in the dashed line of Fig.4a, where the varying phase of the $m=1$ mode is shown - the amplitude of the mode is substantially unchanged from the case without an external momentum source. Second, the imposed bulk plasma flow tends to be slowed down by the macroscopic helical magnetic field, as seen in Fig.4b-c (red profile). **3D self-organized reversed-field pinch helical states.** 3D RFP is characterized by systematic repetition of quasi-single helicity states, with the same dominant mode in between relaxation events, in which a strong redistribution of magnetic energy into kinetic one takes place, thus being a source of momentum. In Fig.5 we evolve 135 modes with $m=0,1,2$ using $\eta_0=10^{-5}$, $v_0=10^{-2}$. We show the temporal behavior of the most relevant modes in Fig.5a, while in Fig.5b we show how the interaction between MHD modes generates a time-oscillating mean plasma flow. As a preliminary result we observe in Fig.5c that a moderate intensity of imposed axial flow (few percent of the Alfvén speed, $v_A \approx 5000$ km/s) leads to a slight enhancement of the helical state, in form of a modest increase of the energy associated to the dominant mode together with a decrease of the energy of secondary perturbations, even in the experimentally relevant region $v_z^{(0,0)}/v_A < 0.01$ (the ratio between the two quantities increases of around 25% with these simulation parameters). **Alfvén waves excitation.** As a further point of novelty (to be discussed in detail in a dedicated publication) we report here to have used our 3D nonlinear MHD modelling tool to study the excitation of Alfvén waves in RFP plasmas: using such a tool allowed not only to compute the spectrum of Alfvénic fluctuations, but also their nonlinear dynamics. In this way we have showed, for the first time, that relaxation events in the RFP excite both compressional and shear Alfvén waves, with features in qualitative agreement with experimental measurements [13].

References:

- 1 Chapman I.T., Hua M.D., Pinches S.D., et al, NF **50**, 045007 (2010)
- 2 Piovesan P., Bonfiglio D., Cianciosa M. et al., NF **57**, 076014 (2017)
- 3 Veranda M., Bonfiglio D., Cappello S., et al., NF **57**, 116029 (2017)
- 4 Pustovitov V.D., NF **51**, 013006 (2011)
- 5 Diamond P.H., McDevitt C.J., Gürçan Ö.D., et al NF **49**, 045002 (2009)
- 6 Fitzpatrick R., PoP **5**, 9, 3325 (1998)
- 7 Bécoulet M., Huysmans G., Garbet X., et al., NF **49**, 085001 (2009)
- 8 Beidler M.T., Callen J.D., Hegna C.C. et al, PoP **24**, 052508 (2017)
- 9 Fitzpatrick R., Hender T.C., Phys Fluids B **3**, 644 (1991)
- 10 Cappello S., Biskamp D., NF **36**, 571 (1996)
- 11 Ebrahimi F., Mirnov V.V., Prager S.C. et al., PoP **15**, 055701 (2008)
- 12 Fitzpatrick R., NF **33**, 1049 (1993)
- 13 Spagnolo S., Zuin M. et al., NF **51** 083038 (2011)

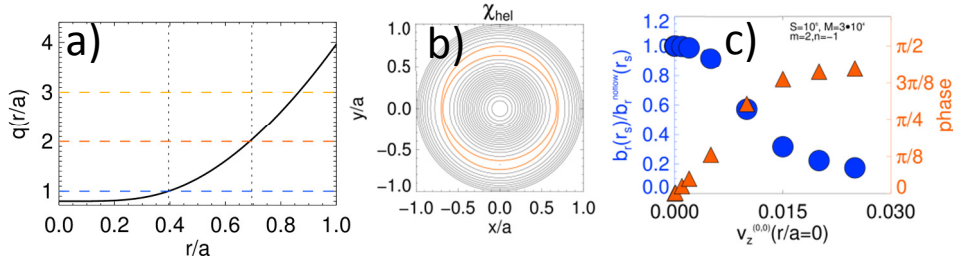


Figure 1: tokamak forced reconnection: effect of increasing bulk rotation. a) Initial safety factor. b) Helical flux function with $m/n=0.5$ and error field amplitude $b_r(a)=10^{-4}$. c) Increasing bulk rotation screens an error field (blue), and changes by $\pi/2$ the phase of the O-point of the island.

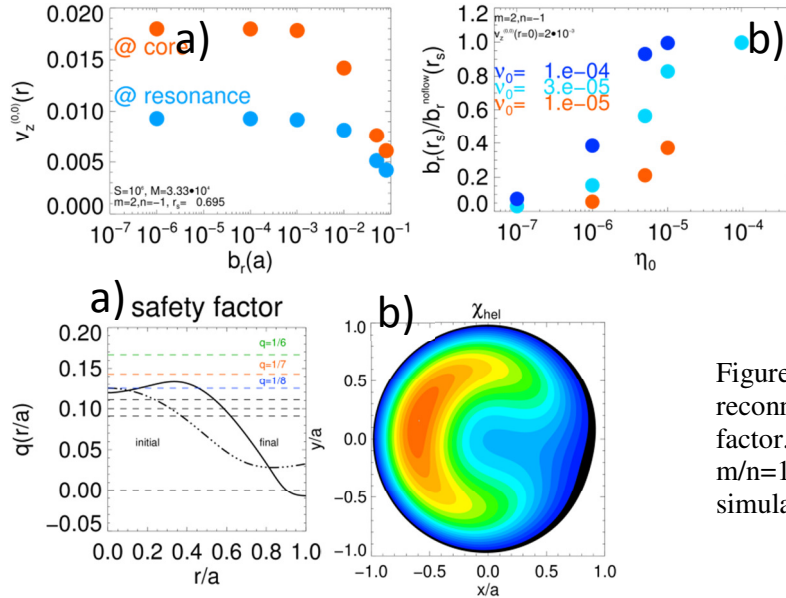


Figure 2: tokamak forced reconnection, effect of MP and dissipation. a) An external error field can slow down bulk plasma rotation. b) Effect of resistivity and viscosity on the amplitude of the reconnected magnetic field.

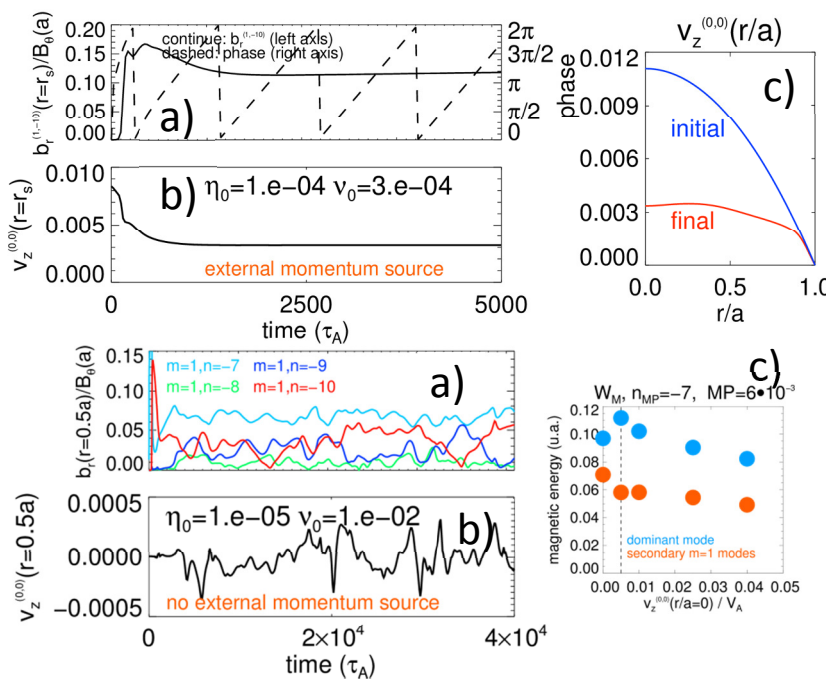


Figure 3: RFP2D tearing reconnection with flow. a) Safety factor. b) Helical flux function with $m/n=10$ at the final snapshot of the simulation in Fig.4.

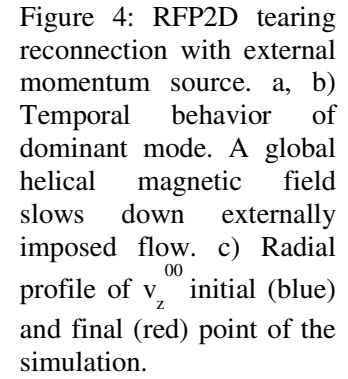


Figure 4: RFP2D tearing reconnection with external momentum source. a, b) Temporal behavior of dominant mode. A global helical magnetic field slows down externally imposed flow. c) Radial profile of $v_z^{(0,0)}$ initial (blue) and final (red) point of the simulation.

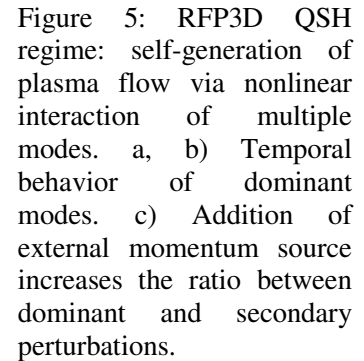


Figure 5: RFP3D QSH regime: self-generation of plasma flow via nonlinear interaction of multiple modes. a, b) Temporal behavior of dominant modes. c) Addition of external momentum source increases the ratio between dominant and secondary perturbations.